

Characterisation of β -lactoglobulin nanoparticles and their binding to caffeine

Article

Accepted Version

Creative Commons: Attribution-Noncommercial-No Derivative Works 4.0

Guo, Y., Harris, P., Kaur, A., Pastrana, L. and Jauregi, P. (2017) Characterisation of β -lactoglobulin nanoparticles and their binding to caffeine. *Food Hydrocolloids*, 71. pp. 85-93. ISSN 0268-005X doi: 10.1016/j.foodhyd.2017.04.027 Available at <https://centaur.reading.ac.uk/71055/>

It is advisable to refer to the publisher's version if you intend to cite from the work. See [Guidance on citing](#).

Published version at: <http://dx.doi.org/10.1016/j.foodhyd.2017.04.027>

To link to this article DOI: <http://dx.doi.org/10.1016/j.foodhyd.2017.04.027>

Publisher: Elsevier

All outputs in CentAUR are protected by Intellectual Property Rights law, including copyright law. Copyright and IPR is retained by the creators or other copyright holders. Terms and conditions for use of this material are defined in the [End User Agreement](#).

www.reading.ac.uk/centaur

CentAUR

Central Archive at the University of Reading

Reading's research outputs online



Characterisation of β -Lactoglobulin nanoparticles and their binding to caffeine

¹Yuchen Guo ²Peter Harris, ³Lorenzo Pastrana, ^{1*}Paula Jauregi

¹Department of Food and Nutritional Sciences. University of Reading, Whiteknights, Reading, RG6 6AP, United Kingdom.

²Centre for Advanced Microscopy, University of Reading, Whiteknights, Reading, RG6 6AP, United Kingdom

³INL - International Iberian Nanotechnology Laboratory, Av. Mestre José Veiga s/n, 4715-330 Braga Portugal

*Corresponding author.

E-mail address: p.jauregi@reading.ac.uk (P.Jauregi)

Address: Department of Food and Nutritional Sciences. University of Reading, Whiteknights, Reading, RG6 6AP, United Kingdom.

Telephone: +44(0)1183788728

1 **ABSTRACT**

2 The production of β -Lg nanoparticles by a simple heat-induced denaturation method
3 without the need to add chemicals was performed at different conditions of pH, and
4 temperature of denaturation. Optimum conditions were set as 0.2 % β -Lg, pH 6 and
5 simply heating at 75°C for 45 minutes. At these conditions, a monodisperse solution
6 with colloidal stability was obtained and the yield of aggregation was over 90%. Shape
7 and size of nanoparticles were determined by Dynamic Light Scattering and by electron
8 microscopy. A monodisperse particle size distribution of spherical shape particles
9 (200nm-300nm diameter) was obtained. The stability of the aggregates towards
10 various types of dissociating buffers was studied. Sodium dodecyl sulphate (SDS) and
11 urea had a strong effect on the size of the nanoparticles, while 2-Mercaptoethanol and
12 Dithiothreitol (DTT) had no significant effect. Therefore hydrogen bonding and
13 hydrophobic interactions were the predominant interactions responsible for the

14 microstructure. Maximum yield of caffeine encapsulation of 13.54% was obtained at
15 caffeine to the β -Lg molar ratio of 50:1. Rapid nanoparticle degradation and increase
16 in polydispersity during the incubation of β -Lg nanoparticles at simulating stomach
17 conditions was observed due to enzymatic attack. Nevertheless, little release of
18 entrapped caffeine was noted. Total release was achieved at intestinal conditions.
19 Finally, the adsorption of caffeine to both native and denatured β -Lg followed a
20 Langmuir adsorption isotherm model and caffeine had three times more affinity for
21 partially denatured β -Lg in nanoparticles than for native protein.

22

23 **Keywords:** Caffeine; nanoparticles; β -Lactoglobulin; simulated digestion,
24 encapsulation.

25 **1. Introduction**

26 Whey is the principal by-product of cheese manufacturing and it represents 85-95% of
27 the initial volume of processed milk with high Chemical oxygen demand (COD) and
28 Biochemical oxygen demand (BOD) values hence its disposal would have a negative
29 environmental impact. The total world production of liquid cheese whey in 2008 was
30 in the region of 187 million metric tons and of this 3.2 million metric tons were
31 industrially utilised and processed into higher added value products such as, whey
32 powder, whey proteins concentrates and whey protein fractions (Afferstsholt & Palmer,
33 2009; C. Baldasso , T.C. Barros, & Tessaro, 2011); the remaining whey is used for
34 animal feed, fertilisers, baby milk powder and some it is just dumped. Whey is a
35 valuable source of proteins (about 0.8-0.9% protein) with high nutritional value and
36 additional biological properties as well as numerous functional properties such as
37 gelation, emulsifying and foaming properties(Jauregi & Welderufael, 2010). The major
38 whey protein, beta-lactoglobulin (β -Lg) which comprises 51 % (w/w) of total protein
39 has very interesting aggregation properties which have been exploited for its application
40 as an encapsulant (Chen, Remondetto, & Subirade, 2006; H. J. Giroux, Houde, &
41 Britten, 2010; Jones, Lesmes, Dubin, & McClements, 2010). This protein is
42 predominantly dimeric at physiological conditions, but dissociates to a monomer at

43 about pH 3 (Tauliera & Chalikian, 2001); its isoelectric point (pI) is 5.13. Four out of
44 its five cysteine residues form two disulfide bridges leaving a free reactive thiol group
45 that appears to be responsible for the formation of covalent aggregates upon heating
46 (Sawyer, 2002). Also β -Lg possess a hydrophobic pocket that when exposed by, for
47 example, heat denaturation forms aggregates by hydrophobic interactions. These
48 aggregation properties can be manipulated by changing temperature, pH, and ionic
49 strength. Under prolonged heating at low pH and low ionic strength, a transparent 'fine-
50 stranded' gel is formed, in which the protein molecules assemble into long stiff fibers
51 and also can produce nanoparticles (Ko & Gunasekaran, 2006).

52 Food protein-based nanoparticles are of great interest because they are Generally
53 Recognised as Safe (GRAS), easy to prepare, no need for chemical cross-linking agents
54 during preparation, better control over size distributions (Chen et al., 2006;
55 Gunasekaran, Ko, & Xiao, 2006). β -Lg is able to aggregate forming nanoparticles that
56 have some technological advantages as an encapsulant for bioactives; among others:
57 inexpensive, food grade and non-toxic material, capable of solubilizing and protecting
58 hydrophobic biologically active molecules in aqueous media as well as capable of
59 retaining sensory qualities, and promote bioavailability of hydrophobic biologically
60 active molecules. In this sense, when electrically charged, β -Lg is also able to ion
61 binding and electrostatic complex formation, self and co-assembly and covalent
62 conjugation (Livney, 2010).

63 In previous works, β -Lg nanoparticles have been applied as carriers for a range of
64 nutraceutical products such as, polysaccharides, pectin, carageenan or chitosan (Chen
65 & Subirade, 2005; Jones et al., 2010; Ron, Zimet, Bargarum, & Livney, 2010; Zimet &
66 Livney, 2009) where β -Lg forms complexes with each of these products. The
67 complexity of method and materials used for the production of such complexes hinders
68 the possibility for scaling up production. On the other hand, simple production steps
69 such as desolvation with ethanol can produce nanoparticles without application of heat,
70 thus making it very feasible for heat-labile bioactive components (Gulseren, Fang, &

71 Corredig, 2012). Nonetheless, usage of organic solvents for food application is still the
72 major drawback for this method (Nicolai, Britten, & Schmitt, 2011).

73 Caffeine is an amphiphilic alkaloid drug that has a strong bioactivity acting as a
74 stimulant drug of the central nervous system. For this reason is considered the most
75 popular legal stimulant consumed in the world, mainly in the form of coffee and tea
76 infusion (Gilbert, 1984). In the last years, several energy drinks containing caffeine
77 have been launched to the market having a great success and customer acceptance
78 (Somogyi, 2010). Unfortunately, caffeine has very bitter taste and unpleasant aftertaste
79 limiting or even excluding their use from many food and drink formulations.
80 Encapsulation of caffeine enables bitterness masking and it can be easily added to food
81 and drink products without changing the flavour or increasing the bitterness level. In
82 addition, encapsulation could provide protection against harsh processing conditions
83 and controlled release.

84 The aim of this study is to investigate the production of β -Lg nanoparticles by a simple
85 heat-induced denaturation method without the need to add chemicals and/or other
86 reagents and to investigate their application to the encapsulation of caffeine. Particles
87 were characterised in terms of size by Dynamic Light Scattering technique,
88 fluorescence and by electron microscopy. Stability to buffers was examined as an
89 indirect measurement of the internal forces responsible for the molecular network
90 within the particles. This led to an improved understanding of the mechanism of
91 aggregate formation and their interactions with caffeine.

92

93 **2. Materials and Methods**

94

95 **2.1. Materials**

96 β -lactoglobulin (β -Lg) from bovine milk, $\geq 90\%$ PAGE lyophilised powder was
97 purchased from Sigma-Aldrich (United Kingdom) for all the experiments. The material
98 used for encapsulation was caffeine (99% purity) obtained also from Sigma-Aldrich
99 (United Kingdom).

100

101

102 **2.2. Methods**

103

104 **2.2.1. Preparation of β -lactoglobulin nanoparticle**

105 The β -lg powder was dispersed in deionized water to make 50 ml 0.2 % w/v β -Lg stock
106 solution and it was stirred magnetically for about two hours at room temperature. This
107 stock solution was stored in a 50ml Falcon tube (VWR International, 525-0403, USA)
108 at 4°C over the whole night to complete hydration. In order to prevent the growth of
109 microorganisms, 200 ppm sodium azide were added.

110 A 5 ml sample from the β -Lg stock solution was added into 15ml a Falcon tube (VWR
111 International, 5250401, USA) and after warming the sample up to room temperature,
112 the pH was measured. Then the pH of the sample was adjusted to 6.0 (except when the
113 pH effect was investigated) using a pH meter (Mettler Toledo, Switzerland) with 0.1M
114 HCL and 0.1M NaOH. After this, the Falcon tube containing the sample was introduced
115 into a water bath (Grant Instrument Ltd., Cambridge, United Kingdom) that had been
116 previously heated at 75 °C. The sample was left for 45 minutes at this temperature
117 except when the effect of heat load was investigated. The temperature of the sample
118 was monitored and it took about 12-14 minutes for the temperature in the samples to
119 reach the water temperature (75 °C). After the set heating time samples were moved to
120 an ice bath for 10 minutes to terminate incubation and the pH of the sample was
121 measured.

122 For experiments where pH effect (from 5.7 to 6.2) was investigated, nanoparticles were
123 produced following procedure described above but initial pH of sample was changed.

124 For experiments where temperature effect was investigated, samples were heated at
125 60 °C and 75°C; all other conditions were kept constant (0.2 % w/w of β -Lg, pH 6 and
126 heating time 75 minutes). For experiments where the heating time (heat load) effect
127 was investigated, nanoparticles were produced following procedure described above at
128 0.2 % w/w of β -Lg, pH 6 and 75°C but at varying heating times: 15, 25, 35, 45, 55, 65
129 and 75 mins.

130

131

132 **2.2.2 Preparation of caffeine encapsulated β -lactoglobulin nanoparticles**

133 The experiment on the encapsulation of caffeine was conducted only with 0.2% (w/v)
134 dispersions. Caffeine (99% purity) was added to the β -Lg dispersions prior to pH
135 adjustment to obtain 10:1, 20:1, 50:1, 100:1, 200:1 caffeine to β -Lg molar ratios. A
136 certain volume of stock caffeine solution (10mg/ml) was mixed with protein samples
137 to achieve 10:1, 20:1 caffeine to β -Lg molar ratios, respectively. The final protein
138 concentration after pH adjustment and caffeine addition was 0.2 % (w/v). Caffeine
139 powder was added into samples to obtain 50:1, 100:1, 200:1 caffeine to β -Lg molar
140 ratios, respectively. Once caffeine was added to the β -Lg solution, the encapsulation
141 method proceeded in the same way as the nanoparticle formation procedure described
142 in section 2.2.1.

143

144 **2.2.3. Particle size distribution**

145 The z-average hydrodynamic diameter of β -Lg nanoparticles was measured by the
146 dynamic light scattering technique using Zetasizer Nano Z (Malvern Instruments Inc.,
147 Malvern, United Kingdom) at $25 \pm 0.1^\circ\text{C}$ and five measurements were taken for each
148 sample. The measurement was determined by considering the refractive index of β -Lg
149 as 1.45 and that of the dispersant medium (deionised water) as 1.33. The z-average
150 mean was calculated from the intensity of light scattered from the nanoparticles, based
151 on Stokes-Einstein equation, which assumes that all particles are spherical. Each sample
152 was measured five times and the mean and standard deviation were determined. In some
153 cases samples were diluted in order to operate at concentrations appropriate for DLS
154 (as indicated by the machine). When samples were incubated with different dissociating
155 buffers the refractive index of these buffers was taken into account: (i) 10M urea,
156 refractive index 1.370 (Warren & Gordon, 1966) (ii) 0.1M Mercaptoethanol, refractive
157 index 1.500 (Sigma-Aldrich, 2017), (iii) 1% (w/v) SDS, refractive index 1.334
158 (Tumolo, Angnes, & Baptista, 2004), (v) 0.1 M DTT, refractive index 1.576 (ChemBK,
159 2017).

160

161

162 **2.2.4. β -lactoglobulin aggregation**

163 The degree of thermal aggregation for β -Lg was determined by separation of denatured
164 β -Lg nanoparticles from native β -Lg using centrifugal ultrafiltration Vivaspin® 20
165 (Sartorius Stedim Biotech, Germany) with 50kDa molecular weight cut-off membrane.

166 To quantify the amount of native and aggregated β -Lg, 5ml of the heated β -Lg solution
167 following the method described in section 2.2.1 was centrifuged at 2000 rpm for 15
168 minutes to collect the retentate as well as the permeate; the retentate and permeate
169 volumes were determined by weight. The concentration of the native β -Lg remained in
170 permeate was determined by the bicinchoninic acid (BCA) method. In brief, 0.1 ml of
171 the permeate solution was added to 2 ml of BCA working reagent (bicinchoninic acid
172 and copper (II) sulphate pentahydrate), followed by incubation at 37°C for 30 min. The
173 reaction solution was measured at 562 nm in an Ultrospec ® 1100 pro UV-vis
174 spectrophotometer (United Kingdom). The percentage of protein aggregated was
175 determined by measuring the total protein in the permeate followed by mass balance on
176 protein.

177

178 **2.2.5. Microscopy method**

179 Environmental Scanning Electron Microscopy (ESEM) was carried out on samples
180 produced at the optimum conditions - 0.2 % β -lactoglobulin, pH 6.0, at 75 °C for 45
181 minutes. The microscope used was a FEI Quanta 600, operated in environmental mode
182 with a water vapour pressure of 822.46Pa, and a specimen temperature of 5°C. The
183 accelerating voltage was 20 kV. One drop of β -lactoglobulin nanoparticles sample was
184 dispersed at the surface of the metal stub of the microscope and was dry at room
185 temperature to ensure to some extent that moisture content was evaporated so that
186 nanoparticles images were easier to capture.

187

188 **2.2.6. Fluorescence measurement of protein solutions**

189 The degree of β -Lg conformational changes on fluorescence emission of tryptophan
190 (Trp) was accessed by fluorescence spectrophotometer with temperature controller
191 (Varian Cary Eclipse, United Kingdom). Fluorescence spectra were obtained after
192 excitation at 280 nm, scanning an emission wavelength range between 290 nm to 510
193 nm, using 5nm excitation and emission slits wavelength. The data was collected by
194 Cary Eclipse software version 2 (Varian Cary Eclipse, United Kingdom). Samples of
195 native β -Lg, heated β -Lg nanoparticles, and caffeine loaded β -Lg nanoparticles were
196 analysed in duplicate at a constant temperature of 20°C.

197

198 **2.2.7. Stability against dissociating buffers**

199 All samples and buffers were filtered by 0.45 μ m filter before the incubation with
200 dissociation buffers. β -Lg nanoparticle dispersions were mixed with equal volume of
201 various dissociating buffers: (i) 10M urea; (ii) 0.1M Mercaptoethanol; (iii) 1% (w/v)
202 SDS; (v) 0.1 M DTT. Dispersions were incubated for 60 min with each buffer and
203 then particle size was measured following the method described in section 2.2.3.

204

205

206 **2.2.8. Zeta potential**

207 Zeta potential of nanoparticle samples was measured by Dynamic light scattering
208 technique using Zetasizer Nano Z in Electrophoretic Light Scattering mode (Malvern
209 Instruments Inc., Malvern, United Kingdom) at $25 \pm 0.1^\circ\text{C}$ and five measurements were
210 taken for each sample. A folded capillary cell (DTS1070) was used to measure the zeta
211 potential. The cell was washed by ethanol and deionised water before each
212 measurement.

213

214 **2.2.9. Caffeine determination by HPLC**

215 An isocratic Reversed phase High Performance Liquid Chromatography (RP-HPLC)
216 equipped with Gilson Model 302 Pump, CE212 Variable wavelength ultraviolet
217 detector and Hewlett Packard 3396A integrator was used to quantify the caffeine
218 concentration contained in permeate. The column used was Ace 5 C18, 25cm \times 4.6mm

219 (Hinchhrom Limited, United Kingdom, particle size 5 μ m), operated at 25 \pm 1 $^{\circ}$ C, the
220 flow rate was 1.0 mL/min, with 50 μ L injection volume, while mobile phase comprised
221 of methanol/water (50/50). Absorption wavelength was selected at 273 nm, which is
222 the maximum wavelength for caffeine. Standard solutions of caffeine were prepared in
223 deionized water in a range of concentrations from 0.001% to 0.01% (w/v). A standard
224 calibration plot was prepared by plotting concentration versus area from which the
225 concentration of caffeine was determined in a range of samples.

226

227 **2.2.10. Encapsulation efficiency**

228 To study the encapsulation efficiency of caffeine into β -Lg nanoparticles, the caffeine
229 encapsulated by the β -Lg particles was separated from free caffeine by centrifugal
230 ultrafiltration membranes of 50KDa MWCO, Vivaspin $^{\circledR}$ 20 (Sartorius Stedim Biotech,
231 Germany). To quantify the amount of free and entrapped caffeine, 5 ml of protein and
232 caffeine solution prepared according to section 2.2.2 was sampled and centrifuged for
233 30 min at 2000 rpm. The retentate was removed carefully by pipette for further analysis
234 while the permeate was used for determination of free caffeine using RP-HPLC. The
235 amount of the entrapped caffeine was determined based on the determination of free
236 caffeine in the permeate and by applying a mass balance. The entrapment efficiency of
237 caffeine was calculated based on the following equation:

238

239

$$240 \text{ Entrapment efficiency (\%)} = \frac{\text{mass of caffeine entrapped}}{\text{original mass of caffeine}} \times 100 \quad (\text{Eq.1})$$

241

242

243

244 **2.2.11. In-vitro gastrointestinal digestion**

245 **Gastric digestion.** The *in-vitro* gastric model protocol was adapted from Zeece *et al.*
246 (2008) and Sarkar *et al.* (2009) with some modifications introduced here. Simulated
247 gastric fluid (SGF) containing 2g of NaCl and 7 mL of HCl, without the addition of

248 pepsin was diluted to 1 L and pH adjusted to 1.2 using 1.0M HCl. Afterwards, 14.93
249 mg of pepsin enzyme was added to 7 ml of SGF and held at 37°C with continuous
250 shaking at 95 rpm in a temperature-controlled water bath (Grant OLS 200, Grant
251 Instrument, United Kingdom) to mimic the conditions in the stomach. The pH and
252 temperature were continuously monitored and controlled.

253

254 Caffeine-loaded β -Lg nanoparticles and pure β -Lg nanoparticles separated from 14 mL
255 suspensions by ultrafiltration (UF) (as described in section 2.2.11) were re-dispersed in
256 14 mL of SGF. Then 7 mL of SGF containing pepsin was added to the mixture to make
257 up a final volume of 21 mL (protein: enzyme ratio 1.87:1 w/w). The mixture was
258 incubated at 37°C for up to 2h and samples were withdrawn at different time intervals
259 for particle size measurement and RP-HPLC analysis. The pH of the mixture was
260 maintained at 1.5 using 1M HCl. The digestion reaction was terminated by raising the
261 pH to 8 with 0.1M NaOH prior to any analysis.

262

263 **Gastrointestinal digestion.** This method was based on a digestion protocol according
264 to Mills et al (2008) and Maccaferri et al (2012) with some modifications. A 15ml
265 dispersion sample containing nanoparticles with and without caffeine was adjusted to
266 pH 2 by using HCl (6M) and mixed with 2.5ml 0.1 M HCl which contained 0.27g
267 pepsin (protein: pepsin ratio 1:9 w/w). The solution was incubated in the 37 °C water
268 bath with a shaker at 95 rpm for two hours. A 0.1 ml sample was taken for analysis of
269 released caffeine by HPLC. Then the rest of the sample was mixed with 12.5ml
270 NaHCO_3 in which 56mg pancreatin (protein: pancreatin ratio 1.07:2 w/w) (P3292,
271 Sigma; 4UPS) and 0.35g bile (protein: bile ratio 1:11.7 w/w) (B 8631, Sigma) were
272 dissolved and the pH of the sample was adjusted to 7 using NaOH (6M). Samples were
273 incubated for three hours. After small intestinal phase incubation samples were filtered
274 through a 0.45 μm filtration unit and analysed by HPLC to determine the caffeine
275 released.

276

277

278 **2.2.12. Caffeine adsorption isotherm**

279 To describe the caffeine adsorption process to β -Lg nanoparticles and native protein the
280 experimental data were fitted to Langmuir adsorption model:

281 (1) $Cad = Cad_{max} \cdot k \cdot C / (1 + k \cdot C)$

282

283 where, Cad is the caffeine adsorbed to β -Lg per protein at equilibrium ($mg\ mg^{-1}$
284 protein), $Cad_{max} \cdot k$ is the maximum amount of caffeine absorbed to β -Lg ($mg\ mg^{-1}$
285 protein), C the concentration of caffeine free in solution at equilibrium ($mg\ ml^{-1}$) and
286 k the adsorption constant ($ml\ mg^{-1}$).

287

288 **2.2.13. Calculations and Statistical Analysis**

289 Calculation of the net charge of β -Lg at different values of pH was performed with the
290 online “protein calculator v3.4” software (<http://protcalc.sourceforge.net>) using the
291 sequence of β -Lg. The results were statistically analysed by analysis of variance using
292 IBM[®] SPSS[®] Statistics version 20.0. Means and standard deviations from at least three
293 measurements carried out on two freshly prepared β -Lg nanoparticles were repeated.
294 The significance level was set at 0.05. Data fitting of experimental data to models was
295 performed with Solver from Excel MS Office 2013 (Microsoft Corporation, Redmond,
296 WA, USA).

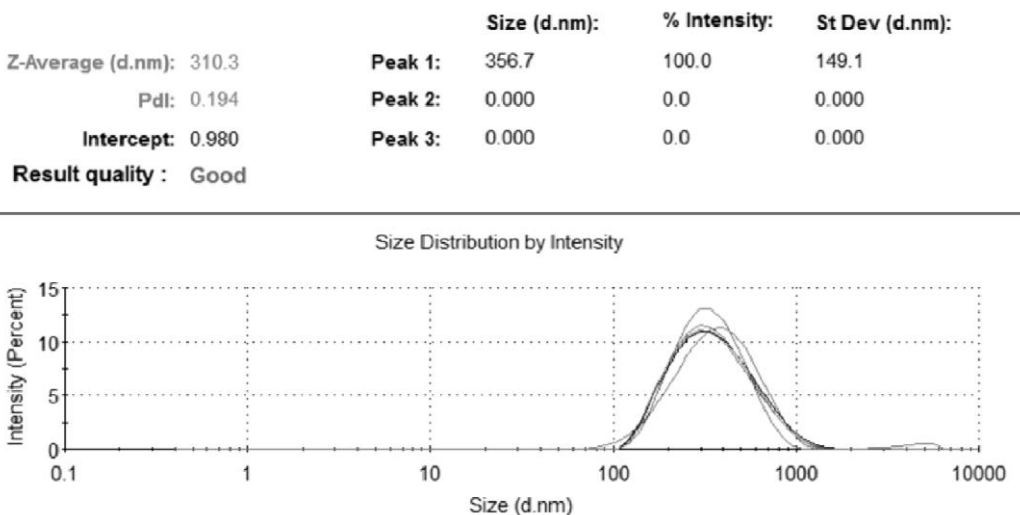
297

298 **3. Results and Discussion**

299 **3.1. Effect of pH, temperature and heat time on β -Lg nanoparticles**

300 Native and heated β -Lactoglobulin (β -Lg) solutions were prepared 0.2% (w/v) and pH
301 adjusted near to their isoelectric point (pH 6.0). All samples appeared to be transparent
302 initially. Also there was only slight turbidity after pH adjustment in agreement with
303 observations previously reported (Chanasattru, Jones, Decker, & McClements, 2009;
304 Mehalebi, Nicolai, & Durand, 2008; Nicolai et al., 2011; Zimet & Livney, 2009). High

305 turbidity after heating at 75°C for 45 minutes appeared to provide a rough quantitative
 306 indication of protein aggregation in the system. A monodisperse particle size
 307 distribution was obtained consistently with particles of an average diameter about 200
 308 nm to 300nm. (See Fig. 1).



309

310 *Figure 1. The example of particle size result by DLS for nanoparticles produced at pH*
 311 *6 and heating at 75 °C for 45 mins.*

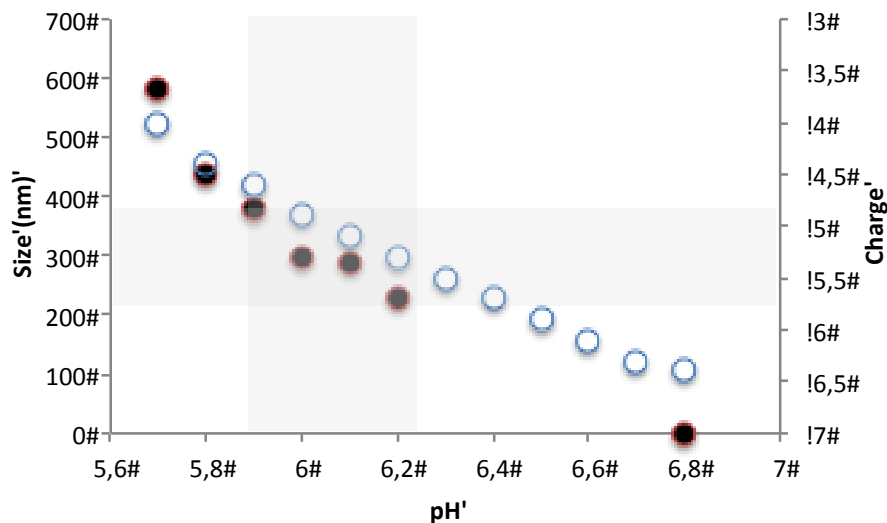
312 **3.1.1. Effect of pH**

313 Near the isoelectric point (pI) of the protein the overall charge is close to zero therefore,
 314 repulsive electrostatic interactions between protein molecules will be minimised and
 315 their aggregation will be promoted. In particular, β -Lg aggregation close to its pI and
 316 under denaturing conditions was reported to produce particulate gels, which were
 317 composed of spherical particles (Donald, 2007).

318 Here we studied the effect of a range of pH's near and above the pI on the particle size.
 319 The pH of the aqueous β -Lg solution (0.2 % w/v) before pH adjustment was 6.8 ± 0.3 .
 320 At this pH, a clear solution was obtained even after heating. This pH was further away
 321 from the pI therefore, strong electrostatic repulsive interactions between protein
 322 molecules hindered their self-aggregation which resulted in reduced turbidity. To test
 323 the effect of pH on protein aggregation and formation of nanoparticles samples were
 324 incubated at pH close to the pI in the range of 5.7 to 6.2 (see figure 2). At pH 5.7 the

325 largest particle size, about 600nm, was recorded and clearly, particle size decreased
 326 with an increase in pH. This indicated that when the pH was close to pI, and the
 327 repulsive electrostatic forces between molecules were minimised, large particles could
 328 be formed. Conversely, when the pH was far from the pI, the repulsive electrostatic
 329 forces were too strong to promote aggregation and consequently smaller particles were
 330 produced. Moreover, according to Tauliera and Chalikian (2001), within pH 5.7-6.2
 331 only a slight change in its tertiary structure occurred but no alteration in secondary
 332 structure. Therefore, the hidden hydrophobic parts of β -Lg were exposed upon pH
 333 adjustment.

334



335

336 *Figure 2. Effect of pH in size and net charge of protein nanoparticles. Size: black*
 337 *circles; protein charge: white circles. Experiments were carried out in duplicate and*
 338 *mean standard deviations were 0.6-9.1 nm*

339

340 Figure 2 shows the relationship between pH and particle size and protein's net charge.
 341 It was concluded that to form nanoparticles with size in the range of 200 nm-350 nm
 342 and colloidal stability the pH should be strictly controlled at 5.9 to 6.2 and protein's net
 343 charge between -5.8 to -4.8. Small changes in pH outside this range leads to small

344 changes in the protein charge but dramatic changes in particle size. So these results
345 highlight the effect of a narrow range of pH close to the protein's pI on particle size.

346

347 **3.1.2. Effect of temperature**

348 The heating temperature was also found to have a significant effect on particle size at
349 constant protein concentration. The turbidity of β -Lg solution heated at 50-60°C
350 remained relatively low but increased steeply from 60-75°C. Reproducible size
351 measurements were difficult to obtain at 65°C and a bimodal distribution was obtained.
352 For instance, the peak of the first distribution produced with 0.2% (w/v) β -Lg was
353 recorded at 3.81 nm, and the sub-population was found at 145 nm. The first population
354 was conjectured to be native β -Lg which is known to have a hydrodynamic radius of
355 around 2.5 nm (Mehalebi et al., 2008). The possible reason of obtaining such population
356 as explained by Bauer *et al.* (Bauer, Carrotta, Rischel, & Ogendal, 2000) is that early
357 aggregation of β -Lg is initiated only at 67.5°C. Significantly larger nanoparticles were
358 formed at 75°C than at 65°C. This suggests that 65°C was not sufficient to induce
359 complete β -Lg chain unfolding to produce nanoparticles in a consistent manner. On the
360 other hand, at 75°C, a monodisperse particle size distribution was obtained consistently
361 with particles of an average diameter about 200 nm.

362 The findings were in agreement with those by Mehalebi et al. (2008) and Gulseren et
363 al. (2012), who found that elevated temperature could accelerate the rate of aggregation
364 to produce larger nanoparticles. Overall the particle sizes reported here are in agreement
365 with those reported by Donato, Schmitt, Bovetto, and Rouvet (2009), who had observed
366 elongated compact aggregates smaller than 200 nm upon heating of 1% (w/v) β -Lg (pH
367 5.9) at 75°C. Also Jones et al. (2010) had produced β -Lg particles ($d < 300$ nm) with
368 good stability to sedimentation as in this study under similar conditions. H.J. Giroux
369 and Britten (2011) reported whey protein nanoparticles in the range of 194 nm produced
370 at pH 5.0 using pH-cycling treatment. According to Jones et al. (2010) optimal
371 conditions for production of β -Lg nanoparticles occurred when the system was heated

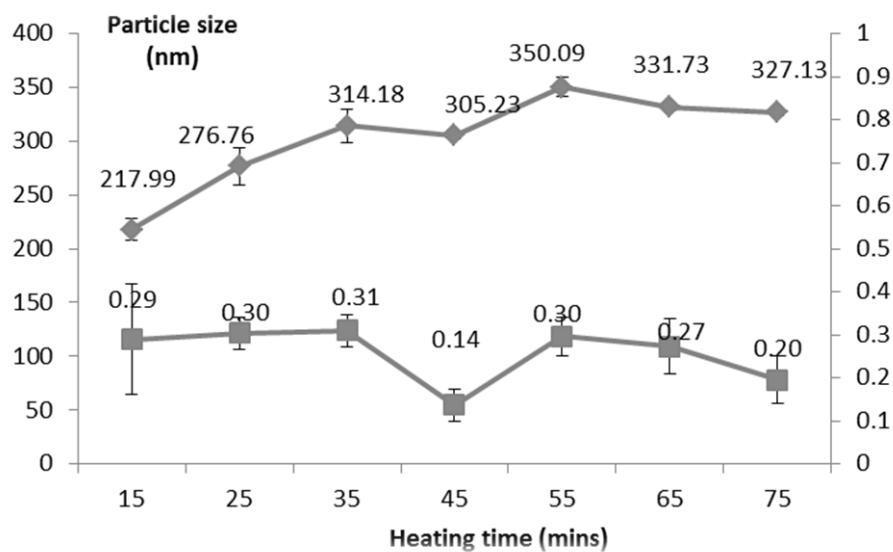
372 above thermal denaturation temperature of β -Lg and at a pH close to its pI which is in
373 agreement with the above findings; these nanoparticles were reported to be irreversible
374 protein aggregates and generally stable towards storage and pH changes.

375 3.1.3. Heating time

376 Besides temperature, the heating time is another factor which has a significant effect on
377 the particle size. Previous studies suggested that long heating time promotes the
378 formation of large aggregates. This was confirmed in the experiments carried out at
379 varying heating times (15 to 75 minutes) but constant temperature, 75 °C (Figure 3);
380 Note that although the water bath was at 75 °C it took about 12-14 mins for the
381 temperature in the dispersion to reach 75 °C.

382

383 Particle size increased from 218 nm to 327 nm in the studied heating time range. The
384 conformation structure changes might happen including the hidden hydrophobic groups
385 at the central cavity and disulphate bonds exposing to the environment and the particles
386 were produced. The polydispersity index (PDI) decreased and had a minimum at
387 45mins. As shown by the low PDI number at this heating time a monodispersion was
388 obtained.



389

390 Fig.3: β -Lg nanoparticle size for continuing heating (15minutes-75mintues). \blacklozenge The β -
391 Lg nanoparticles size; \blacksquare PDI of nanoparticles.

392 In summary, both heating load (combination of temperature and time) and pH were
393 found to be the key operating parameters at constant protein concentration in the
394 production of nanoparticles of a given size. The β -Lg nanoparticles in the range of 200-
395 300 nm were obtained in a consistent and reproducible manner by inducing heat
396 denaturation and aggregation of the protein in an aqueous solution at 0.2%, pH 6.0 and
397 75 °C for 45 minutes. At these conditions, a monodisperse size distribution was
398 obtained and with good reproducibility.

399

400 Protein aggregation may occur due to covalent and non-covalent interactions between
401 unfolded protein molecules. As protein denatures it will unfold to expose the
402 hydrophobic groups as well as the reactive thiol group at Cys¹²¹ which leads to protein
403 molecules interacting via non-covalent interactions (hydrophobic interaction, hydrogen
404 bonding) and covalent interactions (disulphide bonds) to form particles of a given
405 microstructure.(Donato et al., 2009; Havea, Singh, & L.K., 2001). In order to obtain an
406 insight into the physical characteristics of the nanoparticles and their microstructure,
407 the following characterisation study was carried out.

408

409 **3.2 Characterisation of β -Lg nanoparticles**

410

411 **3.2.1 Stability to dissociating buffers**

412 In order to get an insight into the type of the microstructure formed and the main
413 interactions governing its formation the stability of the particles to several buffers was
414 investigated. All samples were filtered by 0.45 μ m filter before the incubation with
415 dissociation buffers. The effect of dissociating buffers was determined based on
416 changes in particle size (Table 1).

417

418

419

420 **Table 1:** Effect of dissociating buffers on nanoparticle diameter (nm). The incubation
421 time with dissociating buffers was 60 minutes.

	<i>Before</i>	<i>10M</i>	<i>1%(W/V)</i>	<i>0.1 M</i>	<i>0.1 M DTT</i>
	<i>incubation</i>	<i>Urea</i>	<i>SDS</i>	<i>2-Mercaptoethanol</i>	
<i>Particle size</i>	<i>173.0±12.5^a</i>	<i>234.2±1.9^b</i>	<i>17.41±8.8^c</i>	<i>176.5±0.9^a</i>	<i>186.1±1.5^a</i>

422 Experiments were carried out in duplicate, mean values with different superscript letters
423 are significantly different at $p < 0.05$, the particle size before incubation is lower than
424 200nm due to the filtration of 0.45 μm filter.

425

426 Sodium dodecyl sulphate (SDS) interacts with proteins via electrostatic interactions and
427 hydrophobic interactions while keeping covalent bonds intact.(Reynolds & Tanford,
428 1970; Roy, Kumar, & Gurusubramanian, 2012). A significant reduction in particle size
429 was observed which demonstrates that hydrophobic interactions are essential to the
430 stabilisation of the microstructure of these particles.

431

432 Urea is a very powerful protein denaturant with the ability to break hydrogen bonds. It
433 is considered that urea acts by breaking down protein hydrogen bonds as it interacts
434 with peptide groups in unfolded proteins by hydrogen bonding. Interestingly, most β -
435 Lg nanoparticles were not disrupted by urea. On the contrary, the particle size increased
436 significantly as demonstrated. The swelling of the nanoparticles could be due to the
437 formation of hydrogen bonds with the water molecules within the particles (Huppertz
438 & de Kruijff, 2008). These results demonstrated the presence of hydrogen bonds within
439 the internal structure of β -Lg nanoparticles.

440

441 2-Mercaptoethanol was added to β -Lg nanoparticle dispersions to cleave disulphide
442 bonds. Interestingly 2-Mercaptoethanol had no significant effect on the size of the
443 nanoparticles, therefore, disulphide bonds were not responsible for the microstructure
444 formation. In order to confirm the above results, another dissociating buffer 0.1 M
445 Dithiothreitol (DTT) was used. DTT is a dissociating buffer, which disrupts disulphide

446 bonds. The nanoparticles were stable during incubation with DTT for 60mins and even
447 after one day (data not shown here). These results confirmed that disulphide bonds were
448 not mainly responsible for the microstructure formation.. Various authors (Alting,
449 Hamer, de Kruif, Paques, & Visschers, 2003; H. J. Giroux et al., 2010; Ko &
450 Gunasekaran, 2006; Mudgal, Daubert, & Foegeding, 2011; Nicolai et al., 2011) have
451 demonstrated the significant role of thiol-disulphide reactions in β -Lg aggregation but
452 the reaction was shown to be favoured at neutral to alkaline pHs. In addition Alting *et*
453 *al.* (Alting et al., 2003) had further ascertained the fact that disulphide bonds did not
454 significantly contribute to the acid-induced aggregation of diluted solutions of whey
455 protein in the initial stage of aggregation. However, partially cross-linked disulphide
456 bonds were found in protein gels kept for a period of time, namely ageing period (Alting
457 et al., 2003; H. J. Giroux et al., 2010; Nicolai et al., 2011). Alting et al. (2003)
458 demonstrated that the formation of disulphide crosslinking was strongly affected by the
459 pH (at pH 5 only 1:3160 sulphur groups is deprotonated and able to initiate
460 thiol/disulphide exchange reactions) and protein concentration (4.5% initial protein
461 concentration was identified as the critical value below which no significant
462 crosslinking may occur). Since the β -Lg nanoparticles produced in this study did not
463 undergo the aforementioned ageing period and the pH and protein concentrations were
464 not favourable to disulphide crosslinking it is reasonable to conclude that disulphide
465 bonds did not actively participate in the formation of the microstructure of the
466 nanoparticles produced in the current study.

467

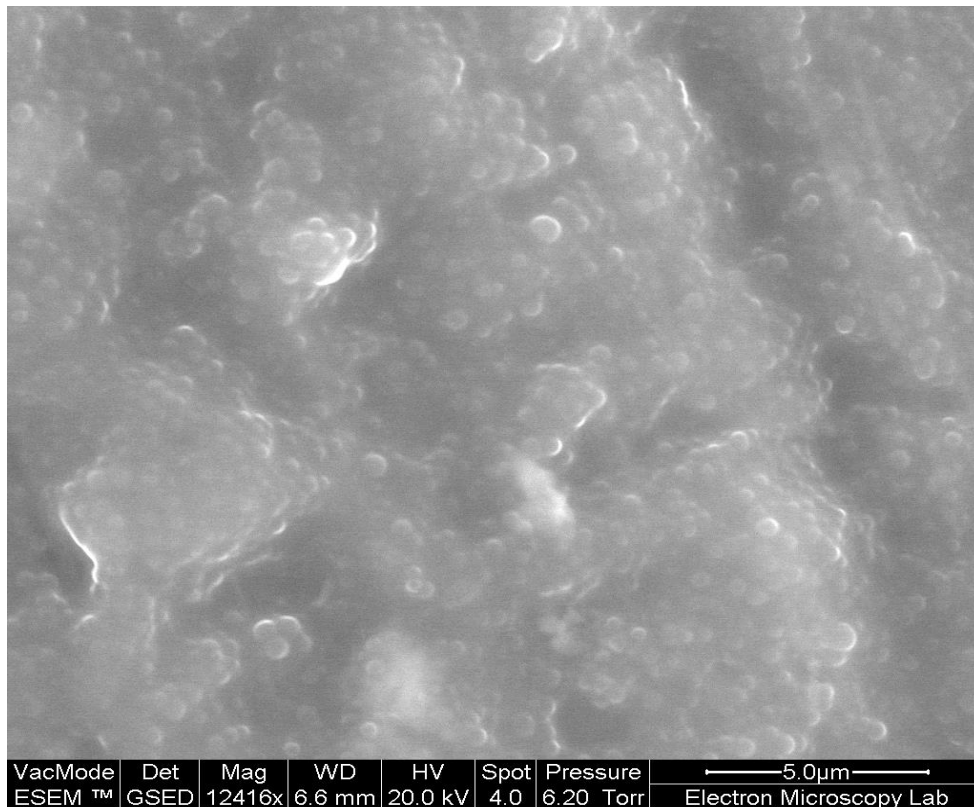
468 In summary, the predominant interactions responsible for the microstructure of the
469 nanoparticles were found to be hydrogen bonding and hydrophobic interactions.
470 Increased hydrogen bonding induces the formation of β -sheets in a protein which, is
471 commonly found in aggregates (Gunasekaran et al., 2006). Hydrophobic interactions
472 also played a major role in the aggregation process of β -Lg as expected since this
473 protein has significant portions of hydrophobic patches, with the exact effective
474 hydrophobicity reported to be 12.2 (Gunasekaran et al., 2006; Hansted, Wejse,

475 Bertelsen, & Otzen, 2011; Ko & Gunasekaran, 2006) and upon denaturation this area
476 will be further exposed.

477

478 3.2.2. Microscope image of nanoparticle

479 To further characterise the microstructure of β -Lg nanoparticles environmental
480 scanning electron microscopy was carried out on samples produced at the optimum
481 conditions (described in 2.2.5).



483 *Figure 4: the ESEM image of β -Lg nanoparticles*

484 The ESEM image in Figure 4 shows spherical aggregates and in the range of sizes of
485 those measured by DLS. This is in agreement with Krebs et al (Krebs, Devlin, &
486 Donald, 2009) who reported the formation of spherical aggregates at the pH close to
487 protein's pI.

488

489 Moreover, the zeta potential of these nanoparticles was determined as the key indicator
490 of the stability of colloidal dispersions. The zeta potential of the β -Lg dispersion was -
491 37.42 ± 2.93 mV which indicated a moderate stable colloidal system.

492

493 **3.2.3 Yield of aggregation of β -Lg**

494 In preliminary filtration experiments with an aqueous solution of β -Lg and a 50KDa
495 ultrafiltration membrane, it was shown that any non-aggregated β -Lg permeated
496 through the ultrafiltration membrane and thus the aggregation yield was determined
497 based on the determination of protein concentration in the permeate by using
498 bicinchoninic acid (BCA) method as described in 2.2.4. Nearly 93% of β -Lg aggregated
499 when heated at 75°C for 45 min. These aggregation yields were similar to those reported
500 by others at higher heating loads (Donato et al., 2009; H. J. Giroux et al., 2010; Moitzi
501 et al., 2011; Mudgal et al., 2011; Schokker, Singh, Pinder, & Creamer, 2000); Giroux
502 *et al.* (H. J. Giroux et al., 2010) reported an aggregation yield of 97.3% after heating
503 1% (w/v) whey protein dispersion at 80°C for 15 min.

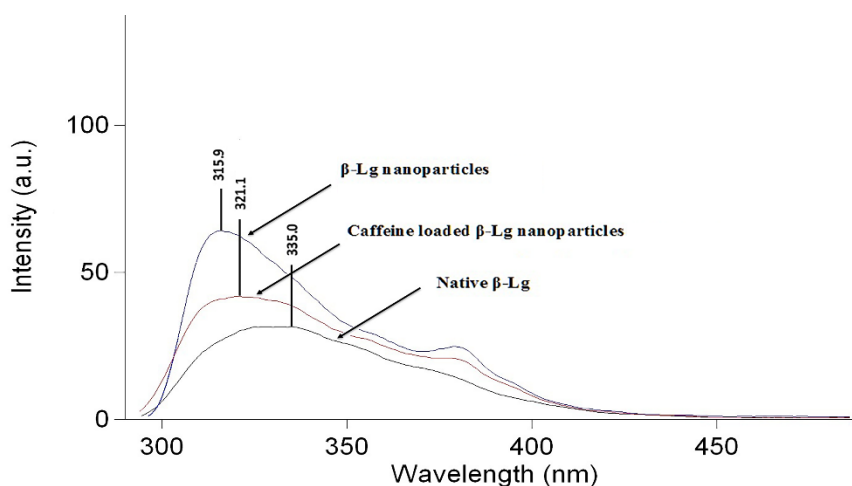
504

505 **3.2.4 β -lactoglobulin conformational changes by fluorescence spectroscopy**

506 The β -Lg contains two tryptophan residues, Trp¹⁹ and Trp⁶¹: Trp¹⁹ within the cavity of
507 β -Lg whereas Trp⁶¹ is located at the surface of the protein molecule and is close to the
508 Cys⁶⁶-Cys¹⁶⁰ disulfide bridge (Qin, Bewley, et al., 1998; Qin, Creamer, Baker, &
509 Jameson, 1998). The X-ray crystallographic image also illustrated that Trp¹⁹ is located
510 in the interior of the β -Lg molecule, which is the major binding point of β -Lg (Sawyer
511 et al., 1985). A mutant β -Lg molecule study helped to prove that Trp¹⁹ was a major
512 fluorophore of β -Lg in the non-polar environment (Creamer, 1995). By the influence
513 of heat, the conformation changed at about 50°C , one of the tryptophans was
514 transferred to a more polar environment accessible to solvent and above 70°C the
515 second tryptophan residue became exposed to solvent. But even at 90°C , the second
516 one was partially buried (Mills, 1976). Therefore in order to investigate conformational
517 changes in β -Lg after heat denaturation and after caffeine encapsulation the

518 fluorescence emission spectra of tryptophan was measured (Fig. 5). An increase in the
519 fluorescence intensity was observed for β -Lg nanoparticles and a fluorescence
520 quenching effect by the caffeine upon binding to the nanoparticles. The increase in
521 fluorescence intensity can be explained based on the exposure of previously buried Trp
522 groups upon heating induced conformational changes in the protein.

523



524

525 *Figure 5: the fluorescence emission changes of native β -Lg, β -Lg nanoparticles and*
526 *caffeine loaded β -Lg nanoparticles.*

527

528 3.2.5. Mechanism of nanoparticle formation

529 Based on previous studies on β -Lg and our observations above the following
530 mechanism of nanoparticle formation is proposed. At neutral pH, β -Lg exists as dimer
531 in aqueous solution. Upon pH adjustment (to pH 6) and heating the dimer dissociates
532 and denatures to reactive monomers. Protein molecules start to unfold and hydrophobic
533 groups are exposed (as shown by fluorescence measurements) which promote
534 intermolecular non-covalent interactions (hydrophobic interactions, and hydrogen
535 bonding) to form particles of a given microstructure as demonstrated by the stability to
536 buffers. Although at these denaturing conditions the reactive thiol group in the protein

537 would get exposed the pH and protein concentration conditions (and lack of aging time)
 538 used in this study did not lead to the formation of disulphide bonds and subsequent
 539 cross-linked gel-like structure. Moreover, the spherical aggregates (as visualised by
 540 ESEM) had a good colloidal stability which was supported by an overall strong negative
 541 charge (-37.42 ± 2.93 mV) measured as zeta-potential.

542

543 3.3. Yield of caffeine encapsulation

544 The yield of caffeine encapsulation increased when caffeine to β -Lg molar ratio
 545 increased reaching a maximum 13.54% at a molar ratio of 50 (mass ratio caffeine to β -
 546 Lg 1:2) (Table 2). Above this maximum, a slow reduction of the percentage of caffeine
 547 encapsulation was observed for higher caffeine to β -Lg molar ratio values. In addition,
 548 caffeine-loaded particles were significantly larger than those without caffeine (over 350
 549 nm). Li *et al.* (Li, Du, Jin, & Du, 2012) and Shpigelman *et al.* (Shpigelman, Cohen, &
 550 Livney, 2012) had also found a similar trend for their EGCG (epigallocatechin-3-gal-
 551 late)-loaded β -Lg nanoparticles.

552

553 Table 2: Caffeine encapsulation. All the encapsulation efficiency results are the
 554 average of three replicates.

<i>Caffeine to β-Lg</i>	<i>10:1</i>	<i>20:1</i>	<i>50:1</i>	<i>100:</i>	<i>200:1</i>
<i>ratio</i>				<i>1</i>	
<i>Encapsulation efficiency (%)</i>	10.25 ± 1.2^b	11.68 ± 3.0^a	13.54 ± 3.3^a	10.07 ± 2.0^c	9.73 ± 0.2^d
<i>Particle size</i>	374.1 ± 5.1^a	366.5 ± 4.7^b	381.7 ± 1.7^c	359.6 ± 3.0^d	356.0 ± 2.6^d

555 Experiments were carried out in triplicate, mean values with different superscript letters
 556 are significantly different at $p < 0.05$

557

558 The same results were plotted as an adsorption isotherm (Figure 6) as it was
 559 hypothesised that caffeine bound (adsorbed) the exterior of the nanoparticles up to
 560 reaching equilibrium concentration. Interestingly it was found that the equilibrium
 561 concentrations of caffeine bound (measured as caffeine mass per protein mass) and
 562 caffeine free in solution followed a Langmuir type isotherm. Parameters of adjustment
 563 of experimental data to Langmuir model are shown in Table 3.

564

565 Table 3: Adjustment of caffeine adsorption to Langmuir model

	<i>Native β-Lg</i>	<i>β-Lg nanoparticles</i>
Cad_{max}	0,103	0,263
k	1,194	0,423
r^2	0,96332	0,96244

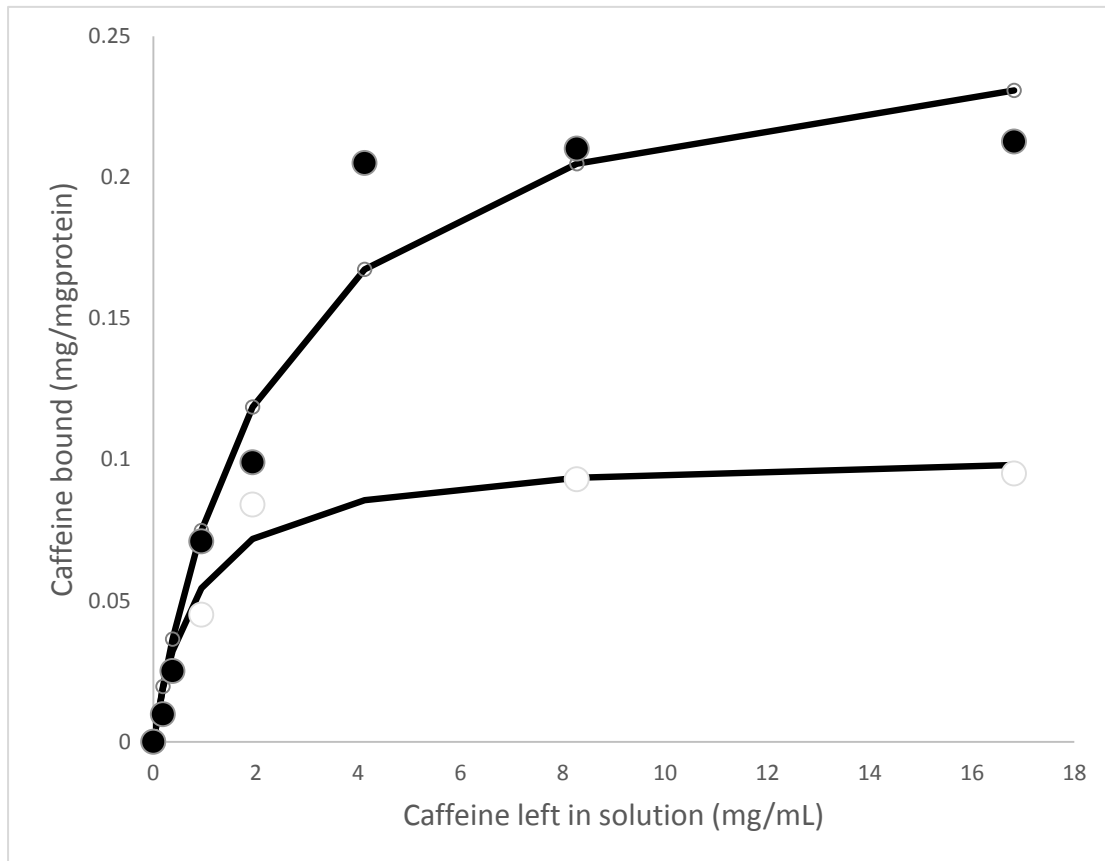
566

567 In the case of nanoparticles, a maximum binding capacity of 0.205 mg caffeine per mg
 568 β -Lg was found which means 19.4 molecules of caffeine per protein. However, when
 569 the same experiments were conducted with native β -Lg the maximum binding capacity
 570 was only 0.084 mg caffeine per mg protein. Additionally, caffeine had three times more
 571 affinity for partially denatured β -Lg in nanoparticles than for native protein.

572 This clearly shows that the conformational change induced in the protein due to heat
 573 denaturation led to an increase in binding capacity.

574

575



576

577 *Figure 6: Isotherm of caffeine encapsulation of native β -Lg (white circles) and the β -*
 578 *Lg nanoparticles (black circles). Lines represent adjustment to Langmuir model.*

579

580

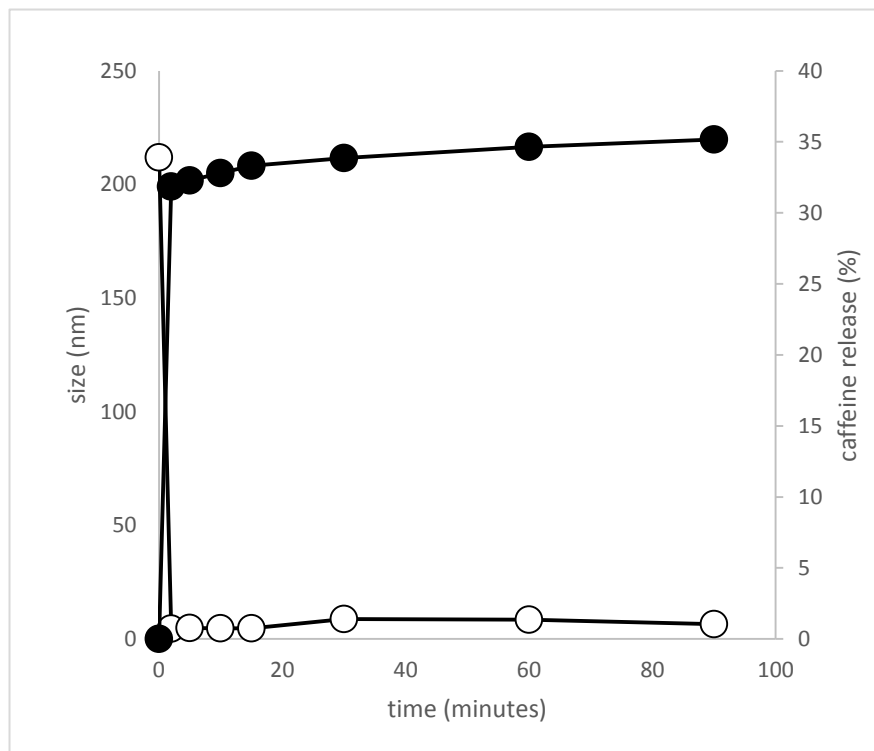
581 **3.5. Simulated gastric digestion**

582 The in-vitro experiment was carried out by suspending the nanoparticles containing
 583 caffeine in simulated gastric fluid (SGF) with pepsin for 120 min under continuous
 584 shaking at 37°C. Conditions of temperature and pH were set equivalent to the normal
 585 gastric digestion conditions (Shpigelman et al., 2012). The protein: enzyme ratio
 586 (1.875:1) used here was similar ratio to that reported in other works (Chen & Subirade,
 587 2005; Sarkar, Goh, Singh, & Singh, 2009; Shpigelman et al., 2012; Zeese, Huppertz, &
 588 Kelly, 2008). It is important to note that optimal ratio that suits the exact physiological
 589 secretion in humans was extremely hard to establish due to the variation in gastric
 590 secretions in different individual's health conditions and food choice (Sarkar et al.,
 591 2009). Various protein: enzyme ratio had been proposed by Kitabatake & Kinekawa
 592 (Kibatake & Kinekawa, 1998), Zeece *et al.* (Zeese et al., 2008); Sarkar *et al.* (Sarkar et

593 al., 2009), and Shpingelman *et al.* (Shpingelman et al., 2012) but all the authors claimed
594 that complete hydrolysis of β -Lg was not achievable at any given pepsin concentration.
595 Therefore, this ratio was chosen here to expose β -Lg nanoparticles to more extreme
596 gastric conditions.

597

598 Upon addition to SGF, the pH of the β -Lg dispersions dropped immediately to around
599 ~ 1.5 to mimic the empty stomach pH and to provide the optimum conditions for
600 hydrolysis by pepsin. Rapid decay of particle size was observed (Figure 7) and during
601 the incubation period polydispersity increased which can be a consequence of the
602 unspecific action of pepsin on the peptide bonds.



603

604 *Figure 7. Black circles: Caffeine release percentage under SGF condition (all results are*
605 *done in duplication.). White circles: Stability of β -Lg nanoparticles at simulating*
606 *stomach conditions. Each of these experiments did in duplicate with standard*
607 *deviations 2.21-3.19% for release and for size 0.80-2.33 nm*

608

609 So particle degradation happened in the first 2 minutes. At this time particle size
610 reduced to 5 nm which corresponds to the average size of a protein dimer (Nicolai et

611 al., 2011; Sakurai , Oobatake , & Goto, 2001) and the size remained as less than 10nm
612 with no significant difference for 60 minutes (Figure 7).

613

614 High Burst effect was observed in the kinetic of caffeine release revealing a common
615 problem in the development of controlled release formulations when low molecular
616 weight compounds are loaded in nanoparticles. This Burst effect seems related with the
617 rapid nanoparticle degradation. In spite of this, high amounts of caffeine were retained
618 in the nanoparticle (68.14% at 2 minutes) and slow and little release of entrapped
619 caffeine was noted, even at the end of incubation (36.4%). Moreover, the gastric
620 digestion applied in the gastrointestinal digestion experiments where lower protein to
621 pepsin ratio was used (1: 9) than in the gastric digestion experiments (1.87:1) (see
622 Methods), led to similar results, 36.71% caffeine released. Furthermore, almost all the
623 caffeine was released after the small intestinal digestion phase (99.22%). Our results
624 agreed with those of Shpigelman et al. (2012) as their β -Lg-EGCG complex managed
625 to preserve 79% of their contents after 180 min of incubation in 1:20 pepsin: protein
626 ratio solution

627 The fact that most of the caffeine is still bound to the protein after the microstructure
628 has been destroyed indicates that the binding of the caffeine to protein is not so
629 dependent on the microstructure but on the protein conformation and the establishment
630 of interactions (most probably hydrophobic and hydrogen bonds) between the protein
631 molecule and the caffeine.

632

633 **Conclusions**

634 One of the main outcomes of this study is that we have developed a simple method that
635 relies in the heat denaturation of β -Lg and leads to the consistent production of
636 nanoparticles of given size (average diameter 200-300) and characteristics with
637 colloidal stability and high yield of aggregation (>93%) at the optimum conditions of
638 pH (6) and heat load (heating at 75 C for 45 mins) which, were found to be the key
639 operating parameters. The characterisation of the nanoparticles by a range of techniques

640 including fluorescence, DLS, and microscopy in combination with the measurement of
641 their stability to buffers led to an improved insight of their formation and their
642 microstructure at the optimum conditions. In summary, heat denaturation led to the
643 protein unfolding, exposure of hydrophobic regions and subsequent formation of
644 protein aggregates by non-covalent intermolecular interactions.

645

646 Maximum encapsulation efficiency of caffeine was 13.54% at 50:1 caffeine to β -
647 Lg molar ratio. Caffeine- β -Lg nanoparticles (~350 nm) were found significantly larger
648 than pure β -Lg nanoparticles (~250 nm). Heating of β -Lg unfolded the non-polar region
649 in the protein and led to an increase in binding of caffeine as compared to native β -Lg.
650 Interestingly, the binding of caffeine to protein followed a Langmuir type isotherm.
651 Both pure β -Lg and caffeine loaded β -Lg nanoparticles exhibited rapid peptic
652 degradation but only 36.4% caffeine was released under these conditions and complete
653 release at intestinal conditions, hence suggesting improved enteric delivery.
654 Furthermore, both the fitting of the experimental results to a binding isotherm and the
655 low release of caffeine even when complete disruption of the microstructure occurred
656 suggest that caffeine binds to the unfolded protein molecule at a maximum ratio of 19
657 molecules of caffeine per molecule of protein. Overall the 'encapsulation' efficiency
658 was slightly better than that obtained with liposomes nanoparticles (3.8% to 9.7%)
659 produced by Pham *et al.* (Pham, Jaafar-Maalej, Charcosset, & Fessi, 2012) utilising
660 phospholipid and cholesterol and less than that obtained with niosomes particles
661 produced from cholesterol and surfactant (30.4%) by Khazaeli *et al.* (Khazaeli,
662 Pardakhty, & Shoorabi, 2007) but with significantly larger vesicle sizes (6-22 μ m).
663 Spontaneous binding of caffeine to β -Lg nanoparticles could open the opportunity for
664 the application of this milk protein as a molecular nano-vehicle to manufacture products
665 fortified with caffeine without intense bitterness that may interfere with the original
666 product flavour. Other potential applications include the binding of bioactives to
667 improve their solubility and/or bioavailability.

668

669

670 **Acknowledgements**

671 Special thanks to Thong Thong Choo who initiated part of this work as an MSc project
672 which formed the basis of the current project.

673

674 **Conflict of interest statement**

675 The author declares that there are no conflicts of interest.

676 **References**

- 677 Afferstsholt, T., & Palmer, S. (2009). Whey proteins: continued market growth despite
678 economic crisis. *NUTRAfoods*, 8, 56-58.
- 679 Alting, A. C., Hamer, R. J., de Kruif, C. G., Paques, M., & Visschers, R. W. (2003). Number of
680 thiol groups rather than the size of aggregates determines the hardness of cold set
681 whey protein gels. *Food Hydrocolloids*, 17, 469-479.
- 682 Bauer, R., Carrotta, R., Rischel, C., & Ogendal, L. (2000). Characterisation and isolation of
683 intermediates in b-lactoglobulin heat aggregation. *Biophysical Journal*, 79, 1030-1038.
- 684 C. Baldasso , T.C. Barros, & Tessaro, I. C. (2011). Concentration and purification of whey
685 proteins by ultrafiltration. *Desalination*, 278(1-3), 381-386.
- 686 Chanasattru, W., Jones, O. G., Decker, E. A., & McClements, D. J. (2009). Impact of cosolvents
687 on formation and properties of biopolymer nanoparticles formed by heat treatment
688 of β -lactoglobulin–Pectin complexes. *Food Hydrocolloids*, 23(8), 2450-2457.
- 689 ChemBK. (2017). DL-Dithiothreitol. Retrieved from <http://www.chembk.com/en/chem/L->
690 [DTT](http://www.chembk.com/en/chem/L-DTT)
- 691 Chen, L., Remondetto, G. E., & Subirade, M. (2006). Food protein-based materials as
692 nutraceutical delivery systems. *Trends in Food Science & Technology*, 17(5), 272-283.
- 693 Chen, L., & Subirade, M. (2005). Chitosan/ β -lactoglobulin core -shell nanoparticles as
694 nutraceutical carriers. *Biomaterials*, 26, 6041-6053.
- 695 Creamer, L. K. (1995). Effect of sodium dodecyl sulfate and palmitic acid on the equilibrium
696 unfolding of bovine β -lactoglobulin. *Biochemistry*, 1995(34), 7170-7176.
- 697 Donald, A. M. (2007). Why Should Polymer Physicists Study Biopolymers? *Journal of Polymer*
698 *Science: Part B: Polymer Physics*, 45, 3257-3262.

699 Donato, L., Schmitt, C., Bovetto, L., & Rouvet, M. (2009). Mechanism of formation of stable
700 heat-induced β -lactoglobulin microgels. *International Dairy Journal*, *19*, 295-306.

701 Gilbert, R. M. (1984). Caffeine consumption. *Prog Clin Biol Res*, *158*, 185-213.

702 Giroux, H. J., & Britten, M. (2011). Encapsulation of hydrophobic aroma in whey protein
703 nanoparticles. *Journal of Microencapsulation (Micro and Nano Carriers)*, *28*(5), 337-
704 343.

705 Giroux, H. J., Houde, J., & Britten, M. (2010). Preparation of nanoparticles from denatured
706 whey protein by pH-cycling treatment. *Food Hydrocolloids*, *24*, 341-346.

707 Gulseren, I., Fang, Y., & Corredig, M. (2012). Whey protein nanoparticles prepared with
708 desolvation with ethanol: characterisation, thermal stability and interfacial behavior.
709 *Food Hydrocolloids*, *29*, 258-264.

710 Gunasekaran, S., Ko, S., & Xiao, L. (2006). Use of whey proteins for encapsulation and
711 controlled delivery applications. *Journal of Food Engineering*, *83*, 31-40.

712 Hansted, J. G., Wejse, P. L., Bertelsen, H., & Otzen, D. E. (2011). Effect of protein-surfactant
713 interactions on aggregation of β -lactoglobulin. *Biochimica Et Biophysica Acta*, *1814*,
714 713-723.

715 Havea, P., Singh, H., & L.K., C. (2001). Characterization of heat-induced aggregates of β -
716 lactoglobulin, α -lactalbumin, and bovine serum albumin in a whey protein
717 concentrate environment. *Dairy Research*, *68*(3), 483-497.

718 Huppertz, T., & de Kruif, C. G. (2008). Structure and stability of nanogels particles prepared by
719 internal cross-linking of casein micelles. *International Dairy Journal*, *18*, 556-656.

720 Jauregi, P., & Welderufael, F. (2010). Added-value protein products from whey extraction,
721 fractionation, separation, purification. *NUTRAfoods*, *9*(4), 13-23.

722 Jones, O. G., Lesmes, U., Dubin, P., & McClements, D. J. (2010). Effect of polysaccharide charge
723 on formation and properties of biopolymer nanoparticles created by heat treatment
724 of β -lactoglobulin-pectin complexes. *Food Hydrocolloids*, *24*, 374-383.

725 Khazaeli, P., Pardakhty, A., & Shoorabi, H. (2007). Caffeine-loaded niosomes: characterisation
726 and *in vitro* release studies. *Drug Delivery*, *14*, 447-452.

727 Kibatake, N., & Kinekawa, Y. (1998). Digestibility of bovine milk whey protein and β -
728 lactoglobulin *in vitro* and *in vivo*. *J. Agric. Food Chem.*, *46*, 4917-4923.

729 Ko, S., & Gunasekaran, S. (2006). Preparation of sub-100-nm β -lactoglobulin (BLG)
730 nanoparticles. *Journal of Microencapsulation*, *23*, 887-898.

731 Krebs, M. R. H., Devlin, G. L., & Donald, A. M. (2009). Amyloid fibril-like structure underlies the
732 aggregate structure across the pH range for β -lactoglobulin. *Biophysical Journal*, *96*,
733 5013-5019.

734 Li, B., Du, W., Jin, J., & Du, Q. (2012). Preservation of (-)-Epigallocatechin-3-gallate Antioxidant
735 Properties Loaded in Heat Treated beta-Lactoglobulin Nanoparticles. *Journal of*
736 *Agricultural and Food Chemistry*, *60*(13), 3477-3484.

737 Livney, Y. D. (2010). Milk proteins as vehicles for bioactives. *Current Opinion in Colloid &*
738 *Interface Science*, *15*(1-2), 73-83. doi:10.1016/j.cocis.2009.11.002

739 Mehalebi, S., Nicolai, T., & Durand, D. (2008). Light scattering study of heat-denatured
740 globular protein aggregates. *International Journal of Biological Macromolecules*, *43*,
741 129-135.

742 Mills, O. E. (1976). Effect of temperature on tryptophan fluorescence of beta-lactoglobulin B.
743 *Biochim Biophys Acta*, *434*(2), 324-332.

744 Moitzi, C., Donato, L., Schmitt, C., Bovetto, L., Gillies, G., & Stradner, A. (2011). Structure of b-
745 lactoglobulin microgels formed during heating as revealed by small-angle X-ray
746 scattering and light scattering. *Food Hydrocolloids*, *25*, 1766-1774.

747 Mudgal, P., Daubert, C. R., & Foegeding, E. A. (2011). Kinetic study of b-lactoglobulin thermal
748 aggregation at low pH. *Journal of Food Engineering*, *106*, 159-165.

749 Nicolai, T., Britten, M., & Schmitt, C. (2011). β -lactoglobulin and WPI aggregates: formation,
750 structure and applications. *Food Hydrocolloids*, *25*, 1945-1962.

751 Pham, T. T., Jaafar-Maalej, C., Charcosset, C., & Fessi, H. (2012). Liposome and niosome
752 preparation using a membrane contactor for scale-up. *Colloids and Surfaces B-*
753 *Biointerfaces*, *94*, 15-21.

754 Qin, B. Y., Bewley, M. C., Creamer, L. K., Baker, H. M., Baker, E. N., & Jameson, G. B. (1998).
755 Structural basis of the Tanford transition of bovine β -lactoglobulin. *Biochemistry*,
756 *1998b*(37), 14014-14023.

757 Qin, B. Y., Creamer, L. K., Baker, E. N., & Jameson, G. B. (1998). 12-Bromododecanoic acid
758 binds inside the calyx of bovine β -lactoglobulin. *FEBS Lett.*, *1998a*(438), 272-278.

759 Reynolds, J. A., & Tanford, C. (1970). Binding of Dodecyl Sulfate to Proteins at High Binding
760 Ratios. Possible Implications for the State of Proteins in Biological Membranes.
761 *National Academy of Sciences*, 66(3), 1002-1007.

762 Ron, N., Zimet, P., Bargaram, J., & Livney, Y. D. (2010). Beta-lactoglobulin-polysaccharide
763 complexes as nanovehicles for hydrophobic nutraceuticals in non-fat foods and clear
764 beverages. *International Dairy Journal*, 20(10), 686-693.
765 doi::10.1016/j.idairyj.2010.04.001

766 Roy, V. K., Kumar, S., & Gurusubramanian, G. (2012). Protein-structure, properties and their
767 separation by SDSpolyacrylamide gel electrophoresis *Sicencevision*, 12(4), 170-181.

768 Sakurai, K., Oobatake, M., & Goto, Y. (2001). Salt-dependent monomer–dimer equilibrium of
769 bovine β -Lg at pH 3. *Protein Science*, 10, 2325-2335.

770 Sarkar, A., Goh, K. K. T., Singh, R. P., & Singh, H. (2009). Behaviour of an oil-in -water emulsion
771 stabilised by β -lactoglobulin in an *in vivo* gastric model. *Food Hydrocolloids*, 23,
772 1563-1569.

773 Sawyer, L. (2002). beta-Lactoglobulin: Properties, structure and function. *Journal of Dairy*
774 *Science*, 85(Supplement 1), 50.

775 Schokker, E. P., Singh, H., Pinder, D. N., & Creamer, L. K. (2000). Heat-induced aggregation of
776 b-lactoglobulin AB at pH= 2.5 as influenced by ionic strength and protein
777 concentration. *International Dairy Journal*, 10, 233-240.

778 Shpigelman, A., Cohen, Y., & Livney, Y. D. (2012). Thermally-induced β -lactoglobulin-EGCG
779 novehicles: loading, stability, sensory and digestive-release study. *Food*
780 *Hydrocolloids*, 29, 57-67.

781 Sigma-Aldrich. (2017). 2-Mercaptoethanol $\geq 99.0\%$ |Sigmaaldrich.com. Retrieved from
782 31 January 2017,
783 <http://www.sigmaaldrich.com/catalog/product/aldrich/m6250?lang=en®ion=GB>

784 Somogyi, L. P. (2010). Caffeine Intake by the U.S. Population.

785 Tauliera, N., & Chalikian, T. V. (2001). Characterization of pH-induced transitions of β -
786 lactoglobulin: ultrasonic, densimetric, and spectroscopic studies. *Journal of Molecular*
787 *Biology*, 314(4), 873-889.

788 Tumolo, T., Angnes, L., & Baptista, M. S. (2004). Determination of the refractive index
789 increment (dn/dc) of
790 molecule and macromolecule solutions by surface plasmon resonance. *Analytical*
791 *Biochemistry*, 333(2), 273-279.

792 Warren, J., & Gordon, J. (1966). On the Refractive Indices of Aqueous Solutions of Urea. . *The*
793 *Journal of Physical Chemistry*, 70(1), 297-300.

794 Zeese, M., Huppertz, T., & Kelly, A. (2008). Effect of high-pressure treatment on in-vitro
795 digestibility of β -lactoglobulin. *Innovative Food Science and Emerging Technologies*, 9,
796 62-69.

797 Zimet, P., & Livney, Y. D. (2009). Beta-lactoglobulin and its nanocomplexes with pectin as
798 vehicles for omega-3 polyunsaturated fatty acids. *Food Hydrocolloids*, 23(4), 1120-
799 1126. doi:10.1016/j.foodhyd.2008.10.008

800